Solid Freeform Fabrication 2016: Proceedings of the 27th Annual International Solid Freeform Fabrication Symposium – An Additive Manufacturing Conference
Reviewed Paper

COST IMPACT OF THE RISK OF BUILD FAILURE IN LASER SINTERING

M. Baumers* and M. Holweg†

*Additive Manufacturing and 3D Printing Research Group, Faculty of Engineering, University of Nottingham, Nottingham, NG7 2RD, United Kingdom
†Saïd Business School, University of Oxford, Oxford, OX1 1HP, United Kingdom

Abstract

While the feasibility of adopting Additive Manufacturing (AM) has been demonstrated in a range of industrial sectors, the total costs associated with the operation of the technology are not fully understood. This study reports the results of a series of build experiments in a controlled environment for the analysis of the total cost of the AM technology variant Laser Sintering (LS). Incorporating a structured representation of the process flow of LS, the developed cost model shows for a LS system of the type EOSINT P100 that the expected cost impact of build failure has a substantial effect, responsible for a share of up to 38% of total costs. The analysis further demonstrates that, due to the adverse effects of such ill-structured costs, the cost efficient level of build volume utilization is sub-maximal. This result is discussed in the context of the operational reality of using LS technology and the availability of economies of scale.

Introduction

The progressing diffusion of Additive Manufacturing (AM) is providing significant scope for manufacturing innovation. The technology is regarded as an opportunity to rethink design, manufacture on demand and generate customized products. The operating principles behind the umbrella term AM range from the thermal fusion of material particles to the exposure to UV radiation of photoreactive monomer resins (Gibson et al., 2014). AM is associated with two generic benefits (Tuck et al., 2008): firstly, AM removes many tooling-related geometrical constraints that are relevant in conventional manufacturing processes (Hague et al., 2003). Secondly, AM permits the realisation of products in small volumes, thereby enabling the manufacture of customized and differentiated designs (Berman, 2012; Eyers et al., 2008). It should be noted, however, that AM is currently limited by a set of generic factors detrimental to the manufacturing of end-use products (Ruffo and Hague, 2007). These factors include deposition speed, materials characteristics, precision, surface quality, process repeatability, and cost at medium to high volumes. As an additional limitation, Huang et al. (2015) identified missing standards for manufacturing applications, particularly relating to material properties.

This paper reports key results of the project “The Economics of 3D Printing: A Total Cost Perspective” (Baumers et al., 2016) funded in the context of the 3DP-RDM feasibility study competition (3DP-RDM, 2016). It addresses the requirement for more realistic AM cost estimation by developing a novel type of model that is able to reflect the expected cost of build failure and part rejection. Shaping the process economics of AM, both aspects have been ignored in previous cost models. To implement the model, this paper adopts an experimental approach relying on a series of build experiments performed on a polymeric EOSINT P100 Laser Sintering (LS) system from equipment manufacturer EOS GmbH in Germany (EOS GmbH, 2015). LS selectively builds up material within a bed of unprocessed powder allowing the user to fill the available build volume

in three dimensions. This characteristic results in a highly parallel process, permitting the manufacture of multiple components (Ruffo et al., 2006). LS is used, for example, in aerospace, automotive, medical, industrial, consumer, and of course, prototyping applications (cf. Wohlers, 2014).

Background and methodology

The goal of strategic cost management is to employ information about cost to determine business strategies for competitive advantage (Shank and Govindarajan, 1993). As demonstrated by Baumers et al. (2013), AM is characterized by the absence of long and complex supply chains normally associated with global mass manufacturing processes. Therefore, AM is likely to improve transparency with regards to production inputs, aiding the development of innovative business strategies.

The seminal AM cost model was implemented by Alexander et al. (1998) and belongs to the class of Activity-Based Costing approaches (cf. Niazi et al., 2006). The model is based on time estimates for multiple process steps, including the time required for the core AM build process. The framework is adaptable to different operating principles found in AM and their effect on build time. Further, Alexander et al. integrated a structure for supporting activities and associated these with pre- and post-processing costs. As noted by Son (1991), however, the cost characteristics of production technology is also shaped by ill-structured aspects. In the AM context, significant ill-structured costs arise from build failure, machine setup and inventory. In an effort to draw such requirements into AM cost models, quality control systems have been incorporated (Schmid and Levy, 2014; Berumen et al., 2010). This research extends such frameworks by systematically investigating the ill-structured cost effect of build failure and part rejection.

To provide a body of data for this research, a series of build experiments was carried out on an EOSINT P100 LS system, which employs a 30W CO_2 laser and was configured to default (factory standard) settings with a layer thickness of 100 μm and using the standard PA2200 material. The build experiments utilized a testing geometry modified for this investigation. As shown in Figure 1a, the geometry features a star shape to maintain packing density at realistic levels, aiming for a packing ratio of around 10% at full capacity utilization, as shown in Figure 1b. The build experiments contained further tensile specimens for the validation of material properties (ISO 527-2:1996, not shown in Figure 1b).

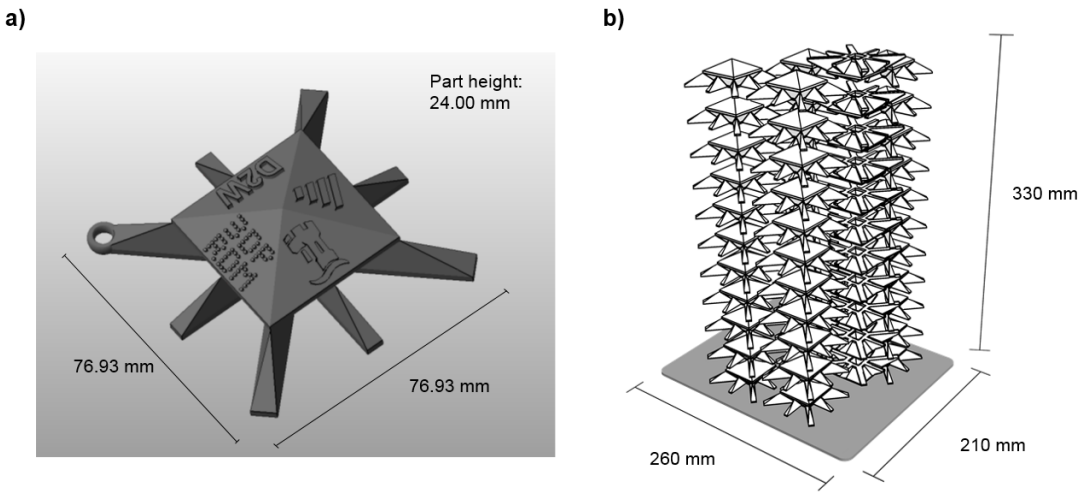

Figure 1: Testing geometry and build volume at full capacity utilization

Exploiting the entire build volume (with a usable Z-height of 330 mm), corresponding to operation at full capacity, would have necessitated extensive and costly builds. Therefore, to allow a sufficient number of repeat experiments in the available time frame, the available machine capacity was artificially restricted to a shallow horizontal band of the build volume. This 30mm 'slice' of build space was filled using a computational build volume packing approach and the data generated during the builds were extrapolated to reflect the system's full Z-height. Overall, 14 build experiments were executed, with 10 builds at full capacity (using the available 30 mm slice) containing 5 parts each. The remaining four build experiments reflect build configurations with sub-normal levels of build volume utilization to gather data on machine operation where the available capacity is not fully employed.

As suggested by Rickenbacher et al. (2013), a central aspect of cost modelling for AM is to consider processes beyond the core manufacturing step. Matching this view, this paper uses a structured representation of the processes required for LS, as shown in Figure 2, identifying process steps performed by the technician (white boxes) and the elements of the AM process itself (grey boxes). Outright build failure events leading to premature build termination and other types of deviation from normal operation leading to part rejection are represented by two decision nodes.

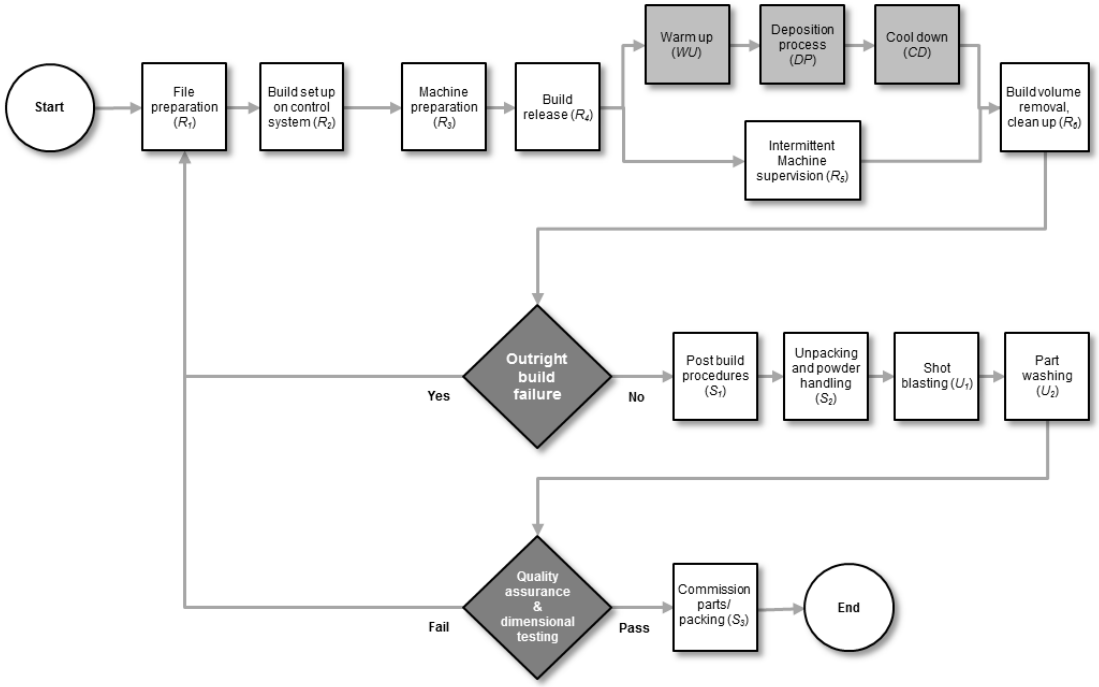

Figure 2: A process map for polymeric Laser Sintering

The durations of the process elements occurring within the AM system (warm up, deposition processes and cool down) were recorded through a digital power meter which also captured the system's energy consumption. The durations of individual process steps in the AM work flow outside the core system were timed by the machine operator and entered into a spreadsheet. The PA 2200 raw material usage was measured by weighing the powder in the build container on digital scales.

Apart from the data originating from the build experiments, the cost model required a range of data from outside sources, such as suppliers and the literature. Table 1 summarizes the collected data points and their respective data sources. The majority of cost data were adapted from previous work by Ruffo et al (2006) and Baumers et al. (2015). Data on the cost of technician labor inputs were obtained from the employer (University of Nottingham). Where cost information was obtained in a currency other than pounds sterling (£), the currency was converted using the exchange rate at the publication date.

Table 1: Summary of external data collected

Cost model element	Data point	Value	Unit	Source
Indirect cost	Production overhead rate	£4.53	/ h	Adapted from Ruffo et al. (2006)
	Admin overhead rate	£0.31	/ h	Adapted from Ruffo et al. (2006)
	Machine purchase	£140,500		Adapted from Baumers et al. (2015)
	Depreciation period	8	Years	Adapted from Ruffo et al. (2006)
	Annual operating time	5,000	H	Adapted from Ruffo et al. (2006)
	Estimated maintenance and consumables	£8,516	/ year	Adapted from Baumers et al. (2015)
	Total machine cost rate	£5.22	/ h	Adapted from Baumers et al. (2015)
	Total indirect cost rate ($\dot{C}_{Indirect}$)	£10.06	/ h	Adapted from Baumers et al. (2015)
Labor cost	Full annual labor costs	£32,420	/ year	-
	Working days net of holiday	228	Days	-
	Total hours worked per year	1653	H	-
	Labor cost rate ($\dot{C}_{Labor}$)	£19.61	/ h	-
Direct cost data	Raw material price	£45.05	/ kg	EOS GmbH (2015)
	Material density, as deposited	0.93	g / cm³	EOS GmbH (2015)
	Energy price	£0.02	/ MJ	Adapted from Baumers et al. (2015)
	Fixed energy consumption per build	25.23	MJ	Adapted from Baumers et al. (2015)
	Energy consumption rate	1,407.50	J / s	-

Results and discussion

In total, 63 test parts (as shown in Figure 1a) and 56 tensile specimens were built, including an additional build to replace rejected test geometries. A nominal part volume of 2521 cm³ (including tensile coupons) was deposited. This required 13.09 kg of new PA2200 powder material, the amount of material was determined by the machine operator. Since two outright build failures occurred during the experiments and one additional build was necessary to replace rejected parts, 17 build experiments were performed in total. Table 2 provides a summary of the performed experimental work.

Table 2: Summary of identified research puzzles and formulated research hypotheses

Experiment no.	1	2	3	4	5	6	7	8
Type	Planned	Planned	Planned	Planned	Planned	Planned	Planned	Repeat build
Capacity utilization	Full	Partial	Partial	Partial	Partial	Full	Full	Full
Number of test geometries included	5	1	2	3	4	5	5	5
Total Z-height (including blank layers and tensile bars)	39.1 mm	35.6 mm	35.6 mm	35.6 mm	35.6 mm	39.1 mm	39.1 mm	39.1 mm
Warm up time (incl. deposition of blank layers and tensile bars)	234 min	204 min	232 min	206 min	204 min	234 min	207 min	190 min
Net normal build time	149 min	106 min	112 min	121 min	132 min	149 min	15 min	150 min
Cool down time	900 min	600 min	1020 min	840 min	600 min	600 min	N/A	840 min
Total build time	1283 min	910 min	1364 min	1167 min	936 min	984 min	N/A	1180 min
Outright build failure	No	No	No	No	No	No	Yes	No
Number of parts rejected	0	0	0	0	0	0	0	1
Material testing failure	No	No	No	No	No	No	No	No

Experiment no.	9	10	11	12	13	14	15	16	17
Type	Planned	Planned	Planned	Repeat build	Planned	Planned	Planned	Planned	Additional build
Capacity utilization	Full	Full	Full	Full	Full	Full	Full	Full	Partial
Number of test geometries included	5	5	5	5	5	5	5	5	3
Total Z-height (incl. blank layers and tensile bars)	39.1 mm	39.1 mm	39.1 mm	39.1 mm	39.1 mm	39.1 mm	39.1 mm	39.1 mm	35.6 mm
Warm up time (incl. deposition of blank layers and tensile bars)	206 min	234 min	164 min	233 min	204 min	199 min	206 min	165 min	Not assessed
Net normal build time	152 min	152 min	70 min	148 min	149 min	151 min	150 min	148 min	Not assessed
Cool down time	960 min	900 min	N/A	720 min	960 min	1080 min	960 min	780 min	Not assessed
Total build time	1318 min	1286 min	N/A	1101 min	1313 min	1430 min	1316 min	1093 min	Not assessed
Outright build failure	No	No	Yes	No	No	No	No	No	No
Number of parts rejected	2	0	0	0	1	0	0	0	0
Material testing failure	No	No	No	No	No	No	No	No	Not assessed

Throughout the series of builds, two separate failure modes were observed. The first kind of failure was outright build failure in which premature stoppage leads to the termination of the build, also assuming that all parts contained in the build volume are lost due to uncontrolled deformation. During the builds, four such outright build failures were recorded, two happening during the build experiments (as listed in Table 2) and two in adjacent builds. This (very limited) dataset allowed the estimation of a mean number of depositable layers between build failures (μ = 4040.71) and the calculation of standard deviation (σ = 3267.95). Clearly, the number of failure-free successively deposited layers N can be greater than the total number of possible layers in each individual build, as limited by build volume Z-height (330 mm, shown in Figure 1b). The results

suggest that undisturbed operation of the LS system is likely to span multiple consecutive builds. To be able to use these estimates in the cost model, two further simplifications are made. Firstly, the probability of build failure is treated as a function P of N, following the normal cumulative distribution function, with distribution mean μ and standard deviation σ:

$$P(N|\mu,\sigma) = \frac{1}{\sigma\sqrt{2\pi}} \int_{-\infty}^{N} e^{\frac{-(t-\mu)^2}{2\sigma^2}} \quad (1)$$

Incorporation of this failure model in the cost model enables the modification of an otherwise deterministic Activity-Based Cost model. The second simplification is to assume that the cost impact of build failure can be characterized by multiplication of the risk free cost model with the inverse of 1- $P(N \mid \mu,\sigma)$.In the schematic of the LS process flow described in Figure 2, the effect of outright build failure is limited to the first decision node. Therefore, only the process steps preceding this node, R_i, are subject by this risk of build failure. The following process elements, S_i and U_i, remain unaffected.

The second failure mode pertains to the rejection of individual parts post completion of the build, due to non-permissible deformation or surface artefacts. Such failure occurs, for example, if foreign objects disturb the deposition process without leading to machine stoppage. The technician assessed the geometries visually and dimensionally for this failure mode. Throughout the build experiments, a total of four test geometries were rejected, one of which was deemed correctable, hence only three replacement parts were manufactured.

This investigation assumes that the risk of part rejection p_{reject} is constant, which can be justified on the basis that the test parts share the same geometry. On the grounds of a planned quantity of 60 test specimens, p_{reject} was estimated at 0.07. This risk affects a larger number of process steps so its decision node occurs later in the schematic work flow shown in Figure 2. As done with outright build failure, this risk characteristic was inserted into the cost model by forming the inverse of its complement.

Following the specification of the failure models, it is clear that the probabilistic term of outright build failure $P(N \mid \mu,\sigma)$ is treated as unrelated to the product geometry. Moreover, this term is treated as unrelated to the fixed probability of part rejection p_{reject}, implying that build configuration does not impact p_{reject}. Both aspects are additional simplifications.

The proposed cost model allocates indirect costs over build time through an indirect cost rate $\dot{C}_{Indirect}$. Additionally, the model adds the labor costs of the process steps in the work flow (partially subject to the risks of failure), ignoring the costs of other equipment outside of the AM system. As described in the process map in Figure 2, outright build failure affects a subset of the overall AM process chain (R_i). Therefore, the total cost of a build $Cost_{Build}$ can be expressed as the sum of the total expected cost of the core AM process, together with surrounding manual operations:

$$Cost_{Build} = \frac{1}{1-P(N)}\left(\dot{C}_{Indirect}T_{build} + C_{Direct} + \sum_{i=1}^{I} R_i\,\dot{C}_{Labor}\right) + \sum_{j=1}^{J} S_j\,\dot{C}_{Labor} + \sum_{k=1}^{K} U_k\,\dot{C}_{Labor}n \quad (2)$$

where T_{Build} is the overall build time (including warm up and cool down), C_{Direct} is the direct cost incurred for raw material and energy, $\dot{C}_{Labor}$ is the labor cost rate, R_i are the timespans attributed

per build of all *i* process elements in the process map affected by the risk of build failure, S_j are the durations attributed per build of all *j* process elements unaffected by this risk, U_k are the durations arising per part of *k* such process elements, and *n* is the total number of product units included in the build. Following the specification of $Cost_{Build}$, the model is broken down to the unit cost level, $Cost_{Unit}$, by assigning the constant probability of post-build part rejection, p_{reject}:

$$Cost_{Unit}(n) = \frac{1}{1 - p_{reject}}\left(\frac{Cost_{Build}}{n}\right) \tag{3}$$

Thus, the new total cost model incorporating risk of failure and ancillary process elements can be expressed as the sum of elements relating to the core build activity, process chain elements subject to risk of build failure and elements not affected by this risk:

$$Cost_{Unit}(n) = \frac{\dot{C}_{Indirect} T_{build} + C_{Direct} + \sum_{i=1}^{I} R_i \dot{C}_{Labor}}{n(1 - p_{reject})(1 - P(N))} + \frac{\sum_{j=1}^{J} S_j \dot{C}_{Labor}}{n(1 - p_{reject})} + \frac{\sum_{k=1}^{K} U_k \dot{C}_{Labor}}{1 - p_{reject}} \tag{4}$$

This unit cost model can be used to explore the behavior of the LS platform as the available build capacity is filled up with test parts. As the main result of this investigation, Figure 3 shows the resulting unit cost function against the number of test geometries *n* contained in the build volume. The ‘saw tooth’ shape of the unit cost function is a result of the extrapolation procedure and therefore carries no meaning. As can be seen, unit cost differs with the level of capacity utilization, from inefficient configurations with a few units in the build volume to a situation fully using up the available build space, as illustrated in Figure 1b. Figure 3 also identifies the level of capacity utilization at each quantity as a build volume utilization ratio which is obtained by dividing the total volume of part geometry over the volume by the useful build volume cuboid. On LS machines, build volume utilization ratios typically range from 5% to 10% in practice.

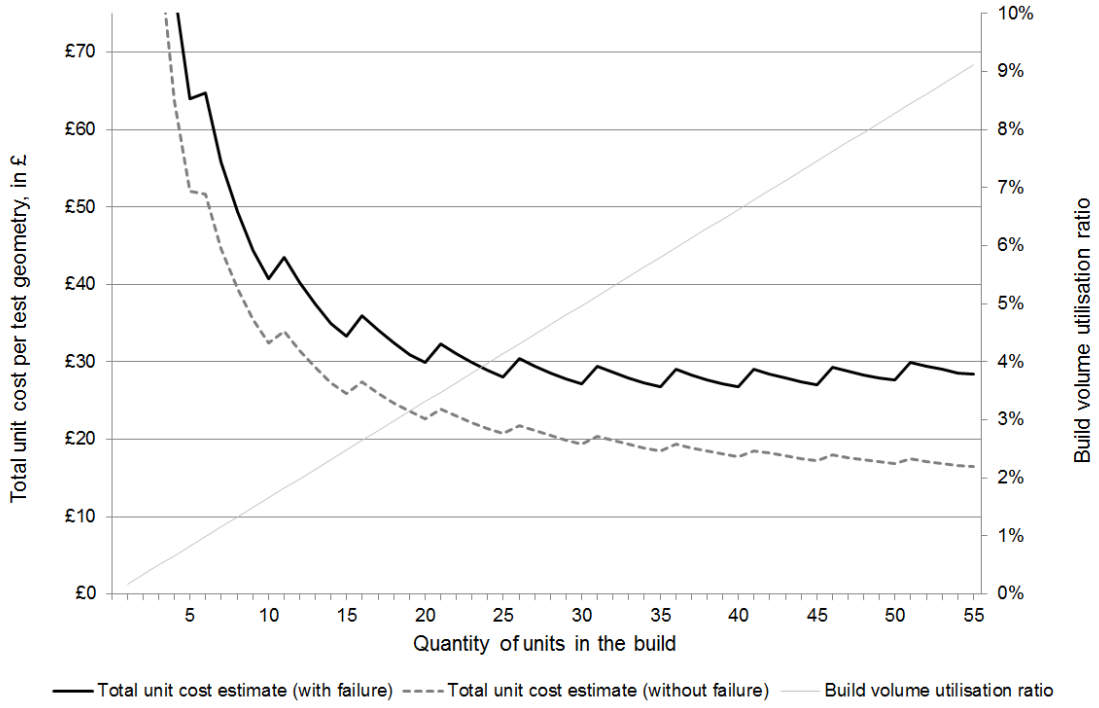

Figure 3: Relationship between unit cost and capacity utilization

Hence, the total cost model proposed in this investigation suggests that (subject to the risk of build failure) unit cost decreases initially but then begins to rise slightly as capacity utilization nears its maximum. The reason for this is an increase of the expected cost of build failure overpowering cost benefits of improved capacity utilization. This can be compared with a model ignoring this risk (Figure 3, dashed line). At full capacity, at a build volume utilization ratio of 9.11%, the proposed model suggests that the specific cost of operating the investigated EOSINT P100 system amounts to £0.89 per cm^3. Due to the inclusion of the risk of build failure, however, the minimum specific cost is observed at a lower capacity utilization rate of 6.62%, at £0.84 per cm^3.

Further insight can be gained by breaking down the total cost into its constituent elements for both levels of capacity utilization, as done in Figure 4 and Figure 5. It is shown that the cost makeup changes with the degree of capacity utilization: the cost component resulting from the risk of build failure, which is obtained by subtracting the costs without risk from the total cost, dominates the process at full capacity utilization (£553.18 or 38%). In the cost efficient configuration, the largest cost contributor is indirect process cost (£377.16) with risk-related costs accounting for £288.22 (or 29%). A further noteworthy point is that labor costs make up only a minor share of the total cost, ranging from £61.20 (or 4.20%) to £49.24 (or 4.93%), respectively.

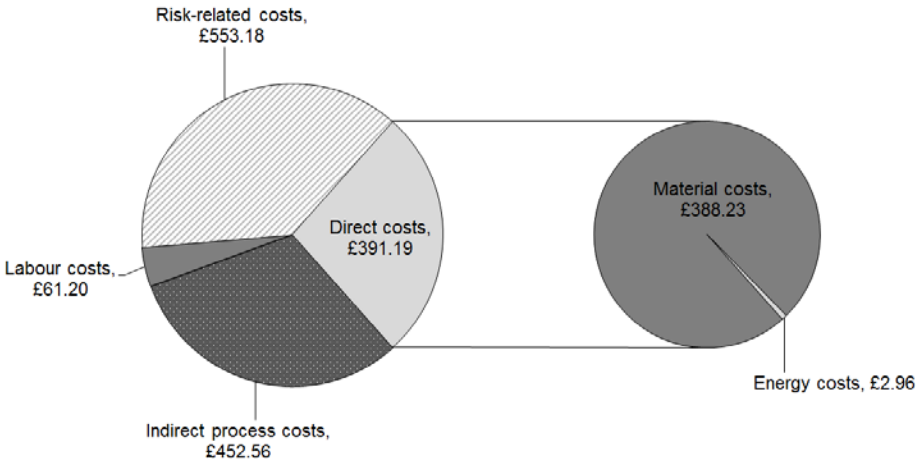

Figure 4: Break down of total cost at full capacity utilization

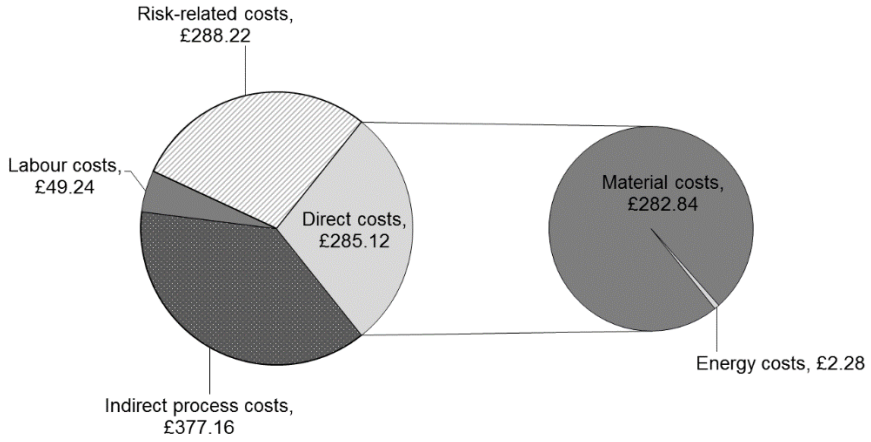

Figure 5: Break down of total cost at minimum cost operation

Results and discussion

The results presented in this paper go beyond existing cost models by exploring a complex relationship between the quantities of parts included within a build volume and the resulting unit cost in AM. As expected, low machine utilization levels will result in high unit cost. However, at high or maximal levels of capacity utilization, the expected cost impact of build failure overpowers the efficiency gains of exploiting the available capacity.

This indicates that the lowest cost configuration may not coincide with full utilization of the available build space, which explains the practice of constraining the Z-height of builds to enable a more efficient process. This aspect is reported to have an impact on the general build volume packing problem encountered in AM (Araujo et al., 2015); it also lends support to cost

models attributing costs to parts by assessing the degree to which they protrude into horizontal bands of otherwise unfilled build space (Rickenbacher et al., 2013). Therefore, such approaches could be used to apportion the expected financial cost of build failure.

In consequence, am technology operators AM face the problem of balancing capacity utilization and risk of build failure. For machine architecture, the results reached in this paper suggest that process stability should be improved such that the expected costs of build failure no longer outweigh efficacy gains originating from the exploitation of the available Z-height. This would allow the costs of fixed process increments, such as warm up and cool down activities to be amortized over a larger number of product units, putting AM users in the position to capitalize on process-level economies of scale.

References

- 3DP-RDM, 2016. 3DP-RDM: Defining the research agenda for 3D printing-enabled re-distributed manufacturing. University of Cambridge. EPSRC Reference: EP/M017656/1

- Alexander, P., Allen, S. and Dutta, D., 1998. Part orientation and build cost determination in layered manufacturing. Computer-Aided Design, 30(5), pp.343-356.

- Araújo, L.J.P., Özcan, E., Atkin, J.A., Baumers, M., Tuck, C. and Hague, R., 2015. Toward Better Build Volume Packing In Additive Manufacturing: Classification Of Existing Problems And Benchmarks. Proceedings of the Solid Freeform Fabrication (SFF) Symposium. The University of Texas at Austin.

- Baumers, M., Tuck, C., Wildman, R., Ashcroft, I., Rosamond, E. and Hague, R., 2013. Transparency Built-in. Journal of Industrial Ecology, 17(3), pp.418-431.

- M. Baumers, M., Tuck, C., and Hague, R., 2015. Selective Heat Sintering Versus Laser Sintering: Comparison of Deposition Rate, Process Energy Consumption and Cost Performance. Proceedings of the Solid Freeform Fabrication (SFF) Symposium. The University of Texas at Austin.

- Baumers, M., Holweg, M., and Rowley, J., 2016. “The Economics of 3D Printing: A Total Cost Perspective”. 3D Printing – Redistributing Manufacturing Project report. Available at www.sbs.ox.ac.uk/sites/default/files/research-projects/3DP-RDM_report.pdf [Accessed 15/07/2016]

- Berman, B., 2012. 3-D printing: The new industrial revolution. Business horizons, 55(2), pp.155-162.

- Berumen, S., Bechmann, F., Lindner, S., Kruth, J.P. and Craeghs, T., 2010. Quality control of laser-and powder bed-based Additive Manufacturing (AM) technologies. Physics procedia, 5, pp.617-622.

- EOS, GmbH, 2015. Corporate website. [Online], available from: www.eos.info/en (Accessed: 24.09.2015).

- Eyers, D.R., Wong, H., Wang, Y. and Dotchev, K., 2008, September. Rapid manufactured enabled mass customisation: untapped research opportunities in supply chain management. In A. Lyons ed.,, Proceedings of the Logistics Research Network Annual Conference, Liverpool, UK (pp. 10-12).

- Gibson, I., Rosen, D. and Stucker, B., 2014. Additive manufacturing technologies: 3D printing, rapid prototyping, and direct digital manufacturing. Springer.

- Hague, R., Campbell, I. and Dickens, P., 2003. Implications on design of rapid manufacturing. Proceedings of the Institution of Mechanical Engineers, Part C: Journal of Mechanical Engineering Science, 217(1), pp.25-30.

- Huang, Y., Leu, M.C., Mazumder, J. and Donmez, A., 2015. Additive manufacturing: Current state, future potential, gaps and needs, and recommendations. Journal of Manufacturing Science and Engineering, 137(1), p.014001.

- Niazi, A., Dai, J.S., Balabani, S. and Seneviratne, L., 2006. Product cost estimation: Technique classification and methodology review. Journal of manufacturing science and engineering, 128(2), pp.563-575.

- Rickenbacher, L., Spierings, A. and Wegener, K., 2013. An integrated cost-model for selective laser melting (SLM). Rapid Prototyping Journal, 19(3), pp.208-214.

- Ruffo, M. and Hague, R., 2007. Cost estimation for rapid manufacturing simultaneous production of mixed components using laser sintering. Proceedings of the Institution of Mechanical Engineers, Part B: Journal of Engineering Manufacture, 221(11), pp.1585-1591.

- Ruffo, M., Tuck, C. and Hague, R., 2006. Cost estimation for rapid manufacturing-laser sintering production for low to medium volumes. Proceedings of the Institution of Mechanical Engineers, Part B: Journal of Engineering Manufacture, 220(9), pp.1417-1427.

- Schmid, M. and Levy, G., 2014. Quality management and estimation of quality costs for additive manufacturing with SLS. ETH-Zürich.

- Shank, J. K., and Govindarajan, V., 1993. Strategic cost management – The new tool for competitive Advantage. Free Press, New York.

- Tuck, C.J., Hague, R.J., Ruffo, M., Ransley, M. and Adams, P., 2008. Rapid manufacturing facilitated customization. International Journal of Computer Integrated Manufacturing, 21(3), pp.245-258.

- Wohlers, T., 2014. Wohlers report 2014: Global reports: Belgium. Wohlers Associates.